

Laser expulsion of an organic molecular nanojet from a spatially confined domain

Masashiro Goto

Nanomaterials Laboratory, National Institute for Materials Science, 3-13 Sakura, Tsukuba 305-0003, Japan

Leonid V. Zhigilei

Department of Materials Science and Engineering, University of Virginia, 116 Engineers Way, Charlottesville, Virginia 22904-4745

Jonathan Hoble

Department of Chemistry, Graduate School of Science, Tohoku University, Sendai, Miyagi 980-8578, Japan

Maki Kishimoto

Advanced Science Research Centre, Japan Atomic Energy Research Institute, 25-1, Mii-Minami-Machi, Neyagawa, Osaka 572-0019, Japan

Barbara J. Garrison

Department of Chemistry, Pennsylvania State University, University Park, Pennsylvania 16802,

Hiroshi Fukumura^{a)}

Department of Chemistry, Graduate School of Science, Tohoku University, Sendai, Miyagi 980-8578, Japan

(Received 2 May 2001; accepted for publication 3 August 2001)

Functional organic molecules have been manipulated into fluorescent features as small as 450 nm on a polymer film using a method derived from laser ablation and laser implantation. The technique utilizes a piezodriver to position a pipette, having a 100 nm aperture and doped at the tip with organic molecules, tens of nanometers above a polymer film. The pipette is subsequently irradiated using 3 ns (full width at half maximum) laser pulses guided down to the tip by a fiber optic. This method of ablation confinement gives fine spatial control for placing functional organic molecules in a designated region and will have applications in optoelectronics. It could also be applied to drug delivery or biotechnology, because in principle, different molecules of diverse function can be manipulated in the same way for various purposes. © 2001 American Institute of Physics. [DOI: 10.1063/1.1407315]

INTRODUCTION

Laser ablation has been proven to be a key player in many fields of engineering.¹ Laser ablation and later, laser implantation, have been used to produce features in polymer films and surfaces limited by the wavelength and beam dimensions of the excitation light employed,^{2–10} however, technology requires the further confinement of patterning processes in order to realize the promise of the potential that nanotechnology offers. For this purpose, we have developed several techniques to reduce the size of patterning that can be produced by laser light.^{7,8,11–13} Laser ablation has been successfully used to manipulate metals¹⁴ and semiconductors,¹⁵ however, it was laser ablative transfer,^{16,17} and later the laser-induced molecular implantation technique,^{2–9,11–13} that proved to be the necessary developments for the manipulation of functional organic molecules. Such molecular manipulation is, of course, necessary if we are to develop the nanoscale molecular devices that are required for the, ever diminishing, size of optoelectronics. Nanoscale molecular manipulation will also have applications in the field of bio-

technology to deliver the desired chemicals to specified regions in a living cell or in biological material such as chromosomes.

In our work on mechanical confinement of the ablation process using glass pipettes having apertures of 100 nm, we have combined laser implantation and laser ablation to advantage and developed a method to create implanted features and clusters having size in the order of hundreds of nanometers. In this way, we hope to pave the way for laser ablation and implantation to enter the realm of nanoengineering. Essentially, we consider the processes of mass transfer, heat transfer, and phase change in the nanodomain to be the necessary fundamental parameters to understand in order to advance this technology, and we consider these parameters in molecular dynamics simulation of the expulsion of molecules from a confined nanopipette.

EXPERIMENT

A conceptual sketch of the method used in this work is shown in Fig. 1. The development of the apparatus used in this study has been previously described,^{12,13} but briefly consists of a pipette having a 100 nm opening positioned 30–50 nm above a polymer film using a shear force feedback controlled piezodriver. A fiber optic guides laser light of a suit-

^{a)} Author to whom correspondence should be addressed; electronic mail: fukumura@orgphys.chem.tohoku.ac.jp

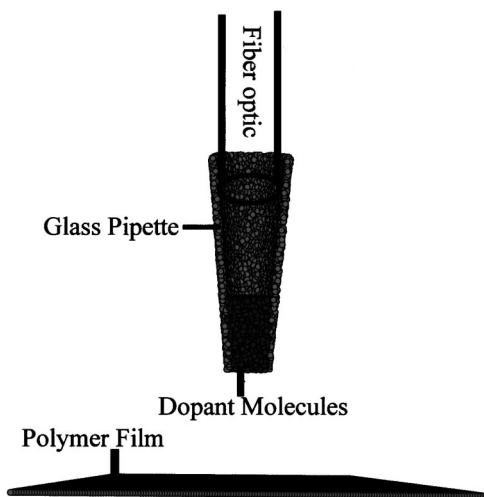
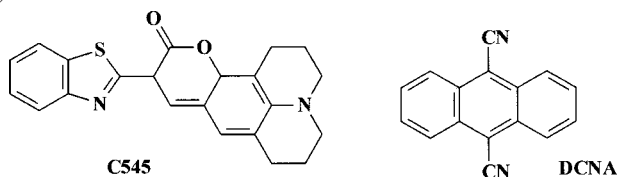


FIG. 1. Conceptual sketch of the apparatus used for nanojet implantation.

able wavelength selected by an optical parametric oscillator into the pipette tip to irradiate molecules [dicyanoanthracene (DCNA) and coumarin 545 (C545), see Diagram 1)



in the form of nanocrystals doped at the pipette tip by slow evaporation from solution. The irradiated crystals are photothermally expelled from the tip as a nanojet of gaseous and molten material that are then quenched on the surface of a polymer film where they either form aggregates or melt into the polymer depending on the laser fluence.

Previously, we described the formation of fluorescent features created using this method having dimensions apparently in the range of several hundreds of nanometers,¹² however, the exact size of the fluorescent feature and the condition of the polymer were unknown, as was the manner in which the light itself propagates inside a nanopipette and the manner of material expulsion. A feature of our apparatus is the ability to interrogate the polymer surface and determine the molecular distribution of ablated material using scanning near-field optical microscopy (fluorescence) and atomic-force microscopy (AFM). An approach to assist our understanding of such nanoscale processes is the simulation of laser-induced molecular expulsion from a doped nanopipette with a breathing sphere molecular dynamics model.

DISCUSSION

To investigate the manner in which light propagates in doped and undoped nanopipettes having tip dimensions of 100 nm, we photographed interference patterns formed by 488 nm light from an Ar⁺ laser that had traveled inside the pipette and then exited forming an image on a transparent plate. These pictures are shown in Fig. 2. Undoped pipettes give a coaxial series of interference fringes starting from the

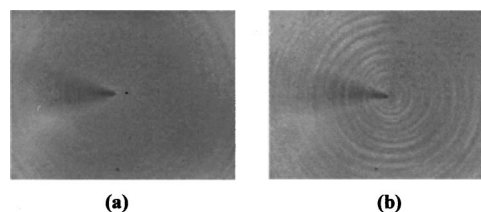


FIG. 2. (a) Transmitted light from a doped pipette tip and (b) from an undoped pipette tip.

very end region of the pipette tip. This necessarily means that light propagates to the end of the tip via partial internal reflection in the walls of the pipette with leaked light forming the interference fringes. Conversely, for C545 doped pipette tips the interference fringes stop short of the end of the tip meaning that the light has been absorbed by the dopant molecules (having a higher refractive index than glass)

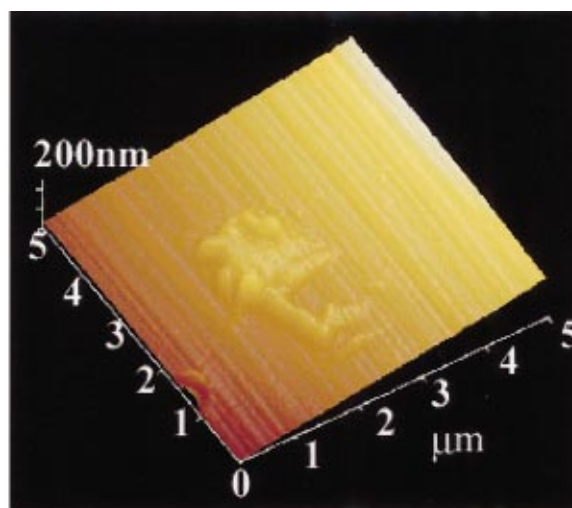


Fig. 3(a)

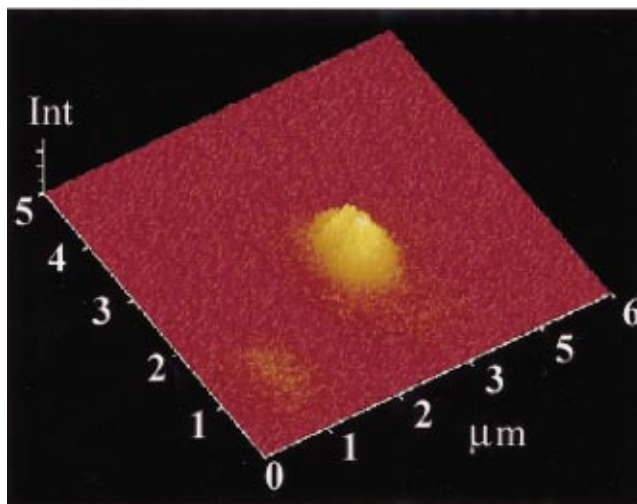


Fig. 3(b)

FIG. 3. (Color) (a) Topographical image of an implanted C545 nanodot created with ten pulses of 200 mJ cm^{-2} (500 nm) laser light. (b) The fluorescence intensity image of the same region.

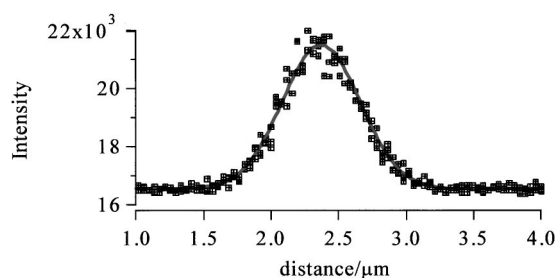


FIG. 4. Fluorescence intensity profile with a Gaussian fit to $K+K_1 \times \exp[-(x-2.36)/0.4]^2$ (solid line).

through the walls of the pipette. This result explains why light can propagate far enough into the tip to excite dopant molecules even though the tip opening, where the molecules are positioned, is of sub-light-wavelength dimensions.

As mentioned above, once excited the dopant molecules are photothermally expelled towards the polymer film, creating fluorescent regions on the polymer surface. The final nature of the dopant molecules and the affected polymer region depends strongly upon the applied laser fluence. After irradiation by ten laser pulses with a wavelength of 500 nm and a fluence of 200 mJ cm^{-2} , fluorescent C545 molecules form fixed dots at the polymer surface with a small degree of thermal damage to the polymer concomitantly occurring. This is shown in Fig. 3. The topographical image corresponds to a maximum deformation height of only 50 nm in the implanted region. As we show in Fig. 4, the fluorescence intensity distribution from the spot of C545 can be approximated as Gaussian, and for a convenient definition of the size of the molecular implantation spot we use the full width at half maximum (FWHM) of the fitted Gaussian distribution. Hence, the size of the smallest implanted (fixed) spot was estimated to be 670 nm.

Figure 4 clearly demonstrates the ability of this method to create nanoregions of functionalized (fluorescent) polymer surfaces with little collateral damage to the polymer occurring and indisputably demonstrates the coupling of ablative implantation techniques to the nanodomain. This is the smallest implanted feature of functional organic molecules created so far.

As a further facet of this technique, we found that using lower laser fluence (140 mJ cm^{-2} , 10 shots, 500 nm) we were even able to make nanoclusters of fluorescent material. These clusters formed on the polymer surface below the pi-

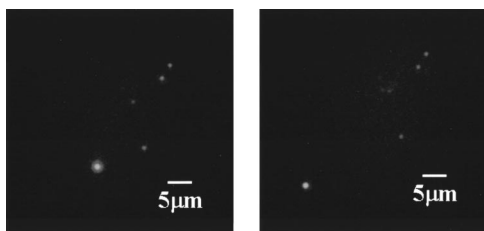


FIG. 5. (a) Series of C545 clusters produced by irradiation with ten pulses of 140 mJ cm^{-2} (500 nm) light. (b) The same polymer region after the lower cluster has been selectively displaced by the AFM tip.

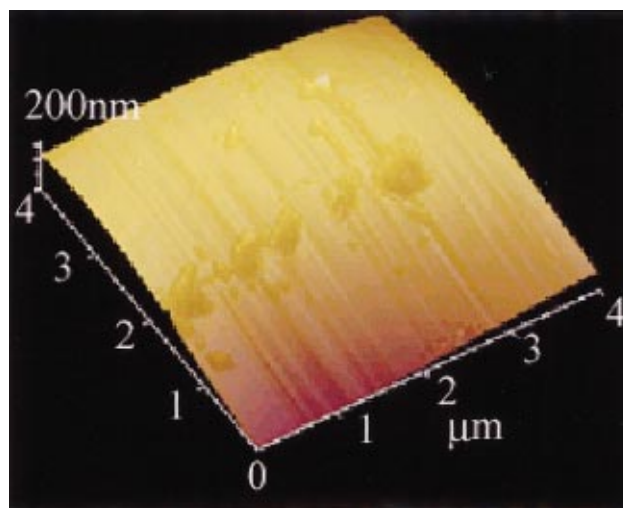


FIG. 6. (Color) Polymer surface after nanoclusters have been displaced showing thermal damage.

pette tip but could subsequently be moved and manipulated with an AFM tip.

Figure 5(a) shows a series of C545 clusters and Fig. 5(b) shows the same polymer region after the lower cluster has been selectively displaced by the AFM tip. Once these movable clusters had been displaced, the polymer surface could be examined for thermal damage. Such a polymer region is shown in Fig. 6. It was found that the area that was under the clusters had become slightly deformed with pits forming where the cluster had landed. The cluster had obviously contained sufficient thermal energy upon arrival at the surface to damage the polymer although C545 molecules from the cluster did not enter the polymer by thermal diffusion as no observable fluorescence was emitted from these same regions after the cluster was removed.

The size of the cluster is obtained again from the FWHM of a Gaussian function fitted to its fluorescence intensity profile, and in the case of the cluster shown in Fig. 7, this corresponds to a cluster diameter of 450 nm.

Here we note three distinct regimes of laser fluence that have been experimentally found:

- (1) Subjection threshold (below 140 mJ cm^{-2}), where the laser fluence was insufficient for molecular transfer to the polymer target surface.
- (2) Nanocluster formation (around 140 mJ cm^{-2}), where the laser fluence was sufficient to eject material, but the material was insufficiently "hot" to become thermally dispersed, adhered to, or mixed with the polymer.

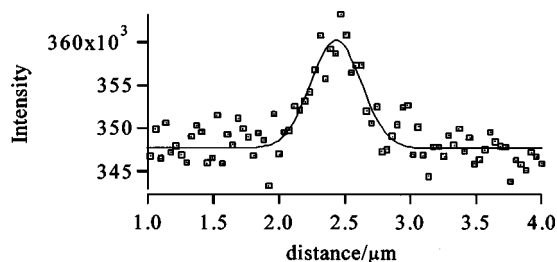


FIG. 7. Fluorescence profile of a movable cluster with a Gaussian fit to $K+K_1 \exp[-(x-2.43)/0.272]^2$ (solid line).

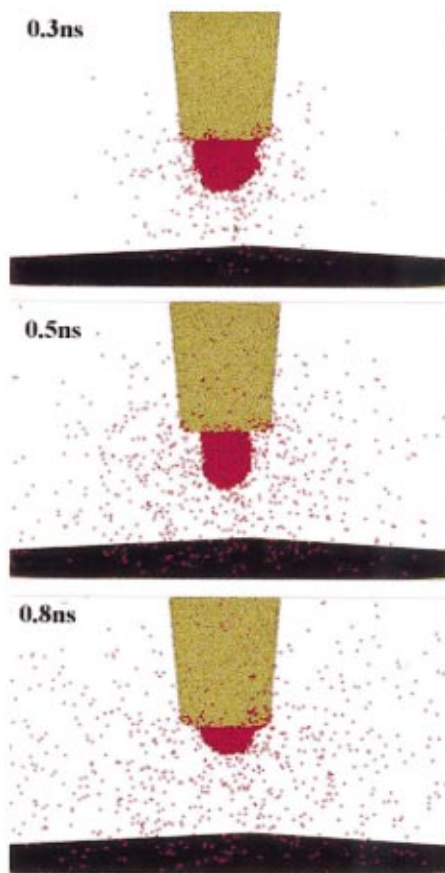


FIG. 8. (Color) Snapshots from the simulations of molecular ejection from an irradiated pipette tip. The laser pulse duration is 100 ps and the energy density deposited by the laser was 2.9 kJ mol^{-1} .

- (3) Implantation (around 200 mJ cm^{-2}), where the ejected material was “hot” enough to become implanted into the surface region of the polymer target.

In order to gain a qualitative understanding of the processes leading to nanojet formation, implantation, and cluster deposition, and to explain the strong fluence dependence and thresholds of the transfer process, we performed a series of simulations of molecular ejection from a doped nanopipette. The simulations were performed using the breathing sphere model¹⁸ that has been developed for molecular dynamics simulations of laser-induced processes in molecular systems. This model has the advantage of addressing the effects of laser irradiation at adequately long scales of time and length while incorporating a realistic description of energy relaxation of individual molecules internally excited by photon absorption.^{19–21} In the present work the parameters for the intermolecular potential in the breathing sphere model are chosen to reproduce the density (1 g cm^{-3}) and the melting point ($250 \text{ }^\circ\text{C}$) of C545 molecular solid and a mass of 374 Daltons is attributed to each molecule.

The initial system in the simulations is similar to the one shown in Fig. 1. Molecular material is located in the tip of a rigid pipette and the pipette is positioned 45 nm above the substrate. The size of the pipette and the pulse duration are scaled down in order to reduce computational time. The opening of the pipette tip of 28 nm and the laser pulse duration of 100 ps were chosen in order to make sure that the simulations are in the same physical regime of thermal

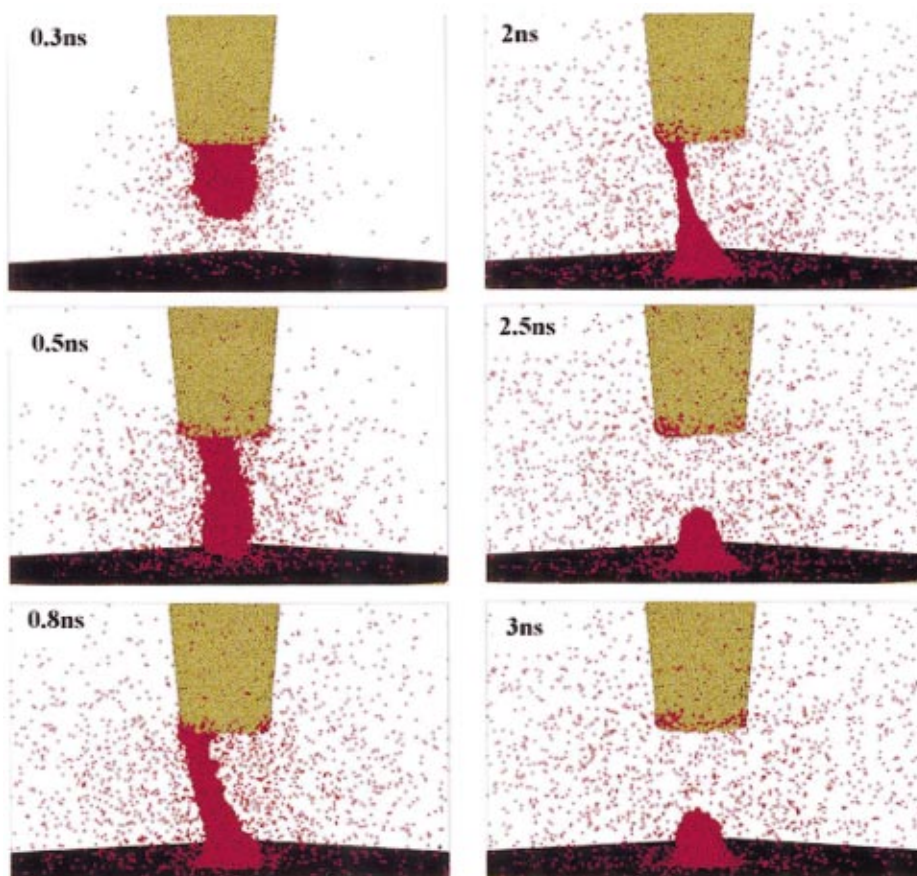


FIG. 9. (Color) Snapshots from the simulations of molecular ejection from an irradiated pipette tip. The laser pulse duration is 100 ps and the energy density deposited by the laser pulse was 3.4 kJ mol^{-1} .

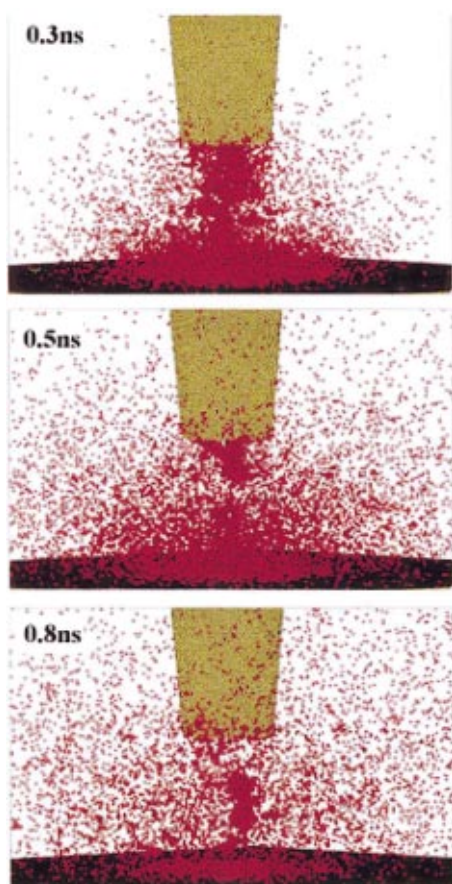


FIG. 10. (Color) Snapshots from the simulations of molecular ejection from an irradiated pipette tip. The laser pulse duration is 100 ps and the energy density deposited by the laser pulse was 5.8 kJ mol^{-1} .

confinement^{19–21} as the experiments. The pulse duration of 100 ps is longer than the time required for relaxation of laser-induced thermoelastic stresses²¹ and photomechanical effects do not play any significant role in the material ejection in the simulations as we assume to be the case in the experiments. It has been demonstrated that in the regime of thermal confinement it is the amount of energy deposited by the laser pulse rather than the pulse duration that controls the desorption/ablation process.^{20–22} The above discussion justifies our comparison between the simulation and experimental data.

Laser irradiation at a wavelength of 500 nm (2.48 eV) is simulated by vibrational excitation of molecules in the pipette tip that are randomly chosen within the duration of the laser pulse. The total number of photons absorbed by the dopant molecules is determined by the incident laser fluence and the absorption coefficient of C545.

“Snapshots” from simulations at three different laser fluences are shown in Figs. 8–10. Even a mere visual inspection of the snapshots reveals a strong fluence dependence of the molecular ejection process, and hence, the final state of the molecular material deposition at the substrate. We find that at low laser fluence molecular material within the tip melts and boils as the temperature of the molecular material in the tip increases above the boiling point. This leads to the expulsion of gas-phase molecules and molecular liquid from

the tip. Interestingly, the simulation shown in Fig. 8 demonstrates that at these lower fluences the expulsion force provided by the release of the gas-phase molecules is not sufficient for the ejection of a liquid droplet and the initial formation of a liquid drop is followed by the retraction of the liquid back into the tip due to the dominant forces of surface tension.

At higher fluences, the laser-induced heating is stronger and the resulting number of gas-phase molecules becomes larger. As a result, a nanojet of molecular liquid and gas is ejected from the tip as shown in Fig. 9. In this simulation the bulk part of the ejected material forms a compact liquid bridge all the way from the tip of the pipette to the substrate. The bridge breaks after 2 ns forming a drop at the substrate. Fast cooling of the droplet due to evaporation and heat conduction to the substrate would lead to the formation of a compact nondispersed nanocluster exactly as we observed experimentally at the subimplantation fluence in Fig. 5.

Further increase of laser fluence leads to stronger heating and explosive boiling of the molecular material in the pipette tip. A hot mixture of gas-phase molecules and small clusters is ejected from the tip at these higher fluences as shown in Fig. 10. Although we do not simulate the actual implantation step in this work and the substrate is represented by a rigid molecular monolayer, we can easily extrapolate that with these high temperatures and velocities of the ejected material (up to 1000 m/s in the front of the ejection plume) a fast transient melting of the exposed polymer surface region and an efficient implantation of the dopant molecules would occur. The experimentally determined size of the implanted dot shown in Figs. 3 and 4 is easily explained when considering the simulation in Fig. 10, which shows that a large area of the polymer substrate is exposed to the hot and mainly gaseous material.

Experimentally, at fluences higher than 200 mJ cm^{-2} , the pipette tip was itself ablated, resulting in glass debris on the polymer surface¹³ and deposition of fluorescent material over a large area covering more than $4 \text{ }\mu\text{m}$. This result can easily be deduced from consideration of the simulations presented here.

In the present case we have investigated nonbiological systems where material is transferred through an air atmosphere to the target, but we envisage many uses in biotechnology where the target film may be a biocompatible polymer or biological tissue doped with a specific molecular substance and where the gap between the target and the nanopipette would be an aqueous solution. In this case quenching of the ejected material would be more rapid and thermal damage would be reduced compared to the present case.

CONCLUSION

We have successfully brought the subjects of laser ablation, laser ablative transfer, and laser implantation into the nanoscale by doping a polymer with functional organic molecules with fine spatial control to create fluorescent implants of 670 nm in diameter and by forming movable fluorescent clusters in the size range of 450 nm. The technology that we have developed will assist in the preparation of molecular

devices to compliment the current semiconductor technology and can have applications in biotechnology to deliver chemicals to designated regions of a biomaterial with submicron resolution.

ACKNOWLEDGMENTS

This work was partly supported by a Grant-in-Aid for Scientific Research (A)(2) from the Japanese Ministry of Education, Science, Sports and Culture (11355035). One of the authors (L.V.Z.) would like to thank the Foreign Researcher Inviting Program of the Japan Atomic Energy Research Institute. This work was partially supported by the NSF through the Materials Research Science and Engineering Center for Nanoscopic Materials Design at the University of Virginia.

- ¹D. Bauerle, *Laser Processing and Chemistry*, 3rd ed. (Springer, Berlin, 2000).
- ²H. Fukumura, H. Kohji, Y. Nagasawa, and H. Masuhara, *J. Am. Chem. Soc.* **116**, 10304 (1994).
- ³K. Saitow, N. Ichinose, S. Kawanishi, and H. Fukumura, *Chem. Phys. Lett.* **291**, 433 (1998).
- ⁴D. M. Karnakis, M. Goto, N. Ichinose, S. Kawanishi, and H. Fukumura, *Appl. Phys. Lett.* **73**, 1439 (1998).
- ⁵D. M. Karnakis, T. Lippert, N. Ichinose, S. Kawanishi, and H. Fukumura, *Appl. Surf. Sci.* **127-129**, 781 (1998).
- ⁶M. Goto, N. Ichinose, S. Kawanishi, and H. Fukumura, *Appl. Surf. Sci.* **138-139**, 471 (1999).
- ⁷J. Hobley, M. Goto, M. Kishimoto, H. Fukumura, H. Uji-I, and M. Irie, *Mol. Cryst. Liq. Cryst.* **345**, 299 (2000).
- ⁸J. Hobley, H. Fukumura, and M. Goto, *Appl. Phys. A: Mater. Sci. Process.* **69**, S945 (1999).
- ⁹M. Goto, S. Kawanishi, and H. Fukumura, *Jpn. J. Appl. Phys., Part 2* **38**, L87 (1999).
- ¹⁰T. Lippert, T. Gerber, A. Wokaun, D. J. Funk, H. Fukumura, and M. Goto, *Appl. Phys. Lett.* **75**, 1018 (1999).
- ¹¹M. Kishimoto, J. Hobley, M. Goto, and H. Fukumura, *Adv. Mater.* (to be published).
- ¹²M. Goto, S. Kawanishi, and H. Fukumura, *Appl. Surf. Sci.* **154-155**, 701 (2000).
- ¹³M. Goto, J. Hobley, S. Kawanishi, and H. Fukumura, *Appl. Phys. A: Mater. Sci. Process.* **69**, S257 (1999).
- ¹⁴I. Zergioti, S. Mailis, N. A. Vainos, P. Papakonstantinou, C. Kalpouzos, C. P. Grigoropoulos, and C. Fotakis, *Appl. Phys. A: Mater. Sci. Process.* **66**, 579 (1998).
- ¹⁵R. Zenobi and V. Deckert, *Angew. Chem. Int. Ed. Engl.* **39**, 1746 (2000).
- ¹⁶I-Yin, S. Lee, W. A. Tolbert, D. D. Dlott, M. M. Doxtader, D. M. Foley, D. R. Arnold, and E. W. Ellis, *J. Imaging Sci. Technol.* **36**, 180 (1992).
- ¹⁷W. A. Tolbert, I.-Y. S. Lee, D. D. Dlott, M. M. Doxtader, and E. W. Ellis, *J. Imaging Sci. Technol.* **37**, 411 (1993).
- ¹⁸L. V. Zhigilei, P. B. S. Kodali, and B. J. Garrison, *J. Phys. Chem. B* **101**, 2028 (1997); **102**, 2845 (1998).
- ¹⁹L. V. Zhigilei and B. J. Garrison, *Appl. Phys. Lett.* **74**, 1341 (1999).
- ²⁰L. V. Zhigilei and B. J. Garrison, *Appl. Phys. A: Mater. Sci. Process.* **69**, S75 (1999).
- ²¹L. V. Zhigilei and B. J. Garrison, *J. Appl. Phys.* **88**, 1281 (2000).
- ²²K. Dreisewerd, M. Schürenberg, M. Karas, and F. Hillenkamp, *Int. J. Mass Spectrom. Ion Processes* **154**, 171 (1996).